

Thermodynamics of Discrete Systems and Martensitic Phase Transition Simulation

A. Berezovski, G.A. Maugin

A thermomechanical approach for the modelling of the phase-transition front propagation in solids is described for the class of thermoelastic phases. This description is based on the balance laws of continuum mechanics in the reference configuration and the thermodynamics of discrete systems. Contact quantities are introduced following the basic concepts of the thermodynamics of discrete systems. The values of the contact quantities are determined within a finite-volume numerical scheme based on a modification of the known wave-propagation algorithm. No explicit expression is used for the kinetic relation governing the phase transition front propagation. All the needed information is extracted from the thermodynamic consistency conditions for adjacent discrete elements. It is shown that the developed model captures the experimentally observed velocity difference which appears because of impact-induced phase transformation.

1 Introduction

Specific features of martensitic phase transformations in solids can be stated as follows (Roytburd, 1995):

1. Martensitic transformations are diffusionless shear transformations;
2. Interfaces between two phases should be coherent and able to move;
3. Martensitic phase transformations can be induced by external loading.

In what follows we consider only stress-induced martensitic phase transformations under dynamic loading. This means that the results of common quasi-static experiments are not suited for the comparison with the computations we performed. The only experimental investigation concerning impact-induced austenite-martensite phase transformations was given by Escobar and Clifton (1993, 1995). In their experiments, Escobar and Clifton used thin plate-like specimens of Cu-14.44Al-4.19Ni shape-memory alloy single crystal. One face of this austenitic specimen was subjected to an oblique impact loading, generating both shear and compression. The conditions of the experiment were carefully designed so as to lead to plane wave propagation in the direction of the specimen surface normal. The orientation of the specimen relative to the lattice was chosen so as to activate only a single variant of martensite. The temperature changes during Escobar and Clifton's experiments are thought to be relatively unimportant. The measurements are taken in the central part of the rear face of the specimen. The ratio of the lateral to the transversal dimensions was chosen so that all the measurements were completed before the arrival of any release wave originating at the lateral faces of the slab. As Escobar and Clifton noted, measured velocity profiles provide several indications of the existence of a propagating phase boundary, in particular, a difference between the measured particle velocity and the transverse component of the projectile velocity. This velocity difference, in the absence of any evidence of plastic deformation, is indicative of a stress induced phase transformation that propagates into the crystals from the impact face.

From another hand side, just the determination of this velocity difference is most difficult from the theoretical point of view. In fact, the above mentioned velocity difference depends on the velocity of a moving phase boundary. Extensive study of the problem of moving phase boundaries (Abeyaratne and Knowles, 1990, 1991, 1994, 1997a; Maugin, 1997, 1998; Maugin and Trimarco, 1995, 1997; Truskinovski, 1987, 1997) shows that the velocity of a moving phase boundary cannot be determined in the framework of continuum mechanics without any additional hypothesis. What continuum mechanics is able to determine is the driving force f_S acting on the phase boundary. The propagation of a phase boundary is thus expected to be described by a kinetic relation between the driving force f_S and the rate V_N , at which the transformation proceeds:

$$V_N = \phi(f_S) \quad (1)$$

where the constitutive function ϕ provides a continuum-level characterization of the micro-mechanisms underlying the transformation process.

Whether impact causes a phase transition depends on the magnitude of the impact velocity. The criterion for the initiation of an austenite-to-martensite phase transition is assumed to be the attainment of a critical value f_* of driving force f_S at the phase boundary (Abeyaratne and Knowles, 1991, 1997a; Fomethé and Maugin, 1997; Maugin, 1997; Maugin and Fomethé, 1997; Truskinovsky, 1997). It is assumed that f_* is a materially determined constant. It is found (Abeyaratne and Knowles, 1991, 1997a) that the kinetic relation and the initiation criterion together single out a unique solution from among the infinitely many solutions that satisfy the jump conditions at discontinuities.

Recently, Abeyaratne and Knowles (1997b) determined, using the experimental data obtained by Escobar and Clifton (1993, 1995), the kinetic relation between the phase boundary velocity and driving force on the basis of the constitutive model they developed. However, the direct comparison between their predictions and experimental data by Escobar and Clifton for the particle velocity cannot be extracted from the paper. Therefore, a theoretical explanation of the particle velocity difference is still needed.

In what follows we describe a thermomechanical approach to the modelling of phase-transition front propagation based on the balance laws of continuum mechanics in the reference configuration (Maugin, 1993) and the thermodynamics of discrete systems (Muschik, 1993). We introduce contact quantities for the description of non-equilibrium states of discrete elements representing the continuous body. The values of contact quantities for adjacent elements are connected by means of thermodynamic consistency conditions (Berezovski et al., 2000). Such conditions are distinct for the homogeneous and heterogeneous cases. The values of contact quantities can be determined within the composite wave-propagation algorithm that was successfully applied for the thermoelastic wave propagation in inhomogeneous media including the case of rapidly varying properties (Berezovski et al., 2000; Maugin and Berezovski, 2000; Berezovski and Maugin, 2001). We exploit different consistency conditions in the bulk and at the interface between different phases. A thermodynamic criterion of the initiation of the phase transition process follows from the simultaneous satisfaction of both homogeneous and heterogeneous thermodynamic consistency conditions at the phase boundary. A critical value of the driving force is determined that corresponds to the initiation of the phase transition process.

Thus, we do not use any explicit expression for the kinetic relation for the phase transition front propagation. We obtain the needed information from the thermodynamic consistency conditions for adjacent discrete elements. It is shown that the developed model captures the experimentally observed particle velocity difference.

2 Uniaxial Motion of a Slab

In order to explain some of the key ideas with a minimum of mathematical complexity, it is convenient to work in an essentially one-dimensional setting. Consider a slab, which in an unstressed reference configuration occupies the region $0 < x_1 < L$, $-\infty < x_2, x_3 < \infty$, and consider uniaxial motion of the form

$$u_i = u_i(x, t) \quad x = x_1 \quad (2)$$

where t is time, x are spatial coordinates, u_i are components of the displacement vector. In this case, we have only three non-vanishing components of the strain tensor

$$\varepsilon_{11} = \frac{\partial u_1}{\partial x} \quad \varepsilon_{12} = \varepsilon_{21} = \frac{1}{2} \frac{\partial u_2}{\partial x} \quad \varepsilon_{13} = \varepsilon_{31} = \frac{1}{2} \frac{\partial u_3}{\partial x} \quad (3)$$

Particle velocities associated with the uniaxial motion (equation (2)) are

$$v_i(x, t) = \frac{\partial u_i}{\partial t} \quad (4)$$

Without loss of generality, we can set $\varepsilon_{13} = 0, v_3 = 0$. Then we obtain uncoupled systems of equations for longitudinal and shear components which express the balance of linear momentum and the time derivative of the Duhamel-Neumann thermoelastic constitutive equation, respectively (Berezovski et al.,

2000; Berezovski and Maugin, 2001):

$$\rho_0(\mathbf{x}) \frac{\partial v_1}{\partial t} = \frac{\partial \sigma_{11}}{\partial x} \quad \frac{\partial \sigma_{11}}{\partial t} = (\lambda(\mathbf{x}) + 2\mu(\mathbf{x})) \frac{\partial v_1}{\partial x} + m(\mathbf{x}) \frac{\partial \theta}{\partial t} \quad (5)$$

and

$$\rho_0(\mathbf{x}) \frac{\partial v_2}{\partial t} = \frac{\partial \sigma_{12}}{\partial x} \quad \frac{\partial \sigma_{12}}{\partial t} = \mu(\mathbf{x}) \frac{\partial v_2}{\partial x} \quad (6)$$

which are complemented by the heat conduction equation

$$C(\mathbf{x}) \frac{\partial \theta}{\partial t} = \frac{\partial}{\partial x} \left(k(\mathbf{x}) \frac{\partial \theta}{\partial x} \right) \quad (7)$$

Here σ_{ij} is the Cauchy stress tensor, ρ_0 is the density, θ is temperature, $C(\mathbf{x})$ is the heat capacity per unit volume by fixed deformation. The dilatation coefficient α is related to the thermoelastic coefficient m , and the Lamé coefficients λ and μ by $m = -\alpha(3\lambda + 2\mu)$. The indicated explicit dependence on the point \mathbf{x} means that the body is materially inhomogeneous in general. These systems of equations, (5) and (6), can be solved separately. We focus our attention on the system of equations (6) for shear components, because the martensitic phase transformation is expected to be induced by shear.

2.1 Jump Relations

The phase transformation is viewed as a deformable thermoelastic body growing at the expense of another deformable thermoelastic body. To consider the possible irreversible transformation of a phase into another one, the separation between the two phases is idealized as a sharp, discontinuity surface \mathcal{S} across which most of the fields suffer finite discontinuity jumps.

Let $[A]$ and $\langle A \rangle$ denote the jump and mean value of a discontinuous field A across \mathcal{S} , the unit normal \mathbf{N} to \mathcal{S} being oriented from the “minus” to the “plus” side:

$$[A] := A^+ - A^- \quad \langle A \rangle := \frac{1}{2}(A^+ + A^-) \quad (8)$$

Let $\tilde{\mathbf{V}}$ be the material velocity of the geometrical points of \mathcal{S} . The material velocity \mathbf{V} is defined by means of the inverse mapping $\mathbf{X} = \chi^{-1}(\mathbf{x}, t)$, where \mathbf{X} denotes the material points (Maugin, 1993)

$$\mathbf{V} := \left. \frac{\partial \chi^{-1}}{\partial t} \right|_{\mathbf{x}} \quad (9)$$

The phase transition fronts considered are homothermal (no jump in temperature; the two phases coexist at the same temperature) and coherent (they present no defects such as dislocations). Consequently, we have the following continuity conditions (Maugin, 1997, 1998; Maugin and Trimarco, 1997):

$$[\mathbf{V}] = 0 \quad [\theta] = 0 \quad \text{at } \mathcal{S} \quad (10)$$

Jump relations associated with the conservation laws in the bulk are formulated according to the theory of weak solutions of hyperbolic systems. Thus the jump relations associated with the balance of linear momentum and balance of entropy read (Maugin, 1997, 1998; Maugin and Trimarco, 1997)

$$V_N [\rho_0 v_2] + [\sigma_{12}] = 0 \quad V_N [S] - \left[\frac{k}{\theta} \frac{\partial \theta}{\partial x} \right] = \sigma_S \geq 0 \quad (11)$$

where $V_N = \tilde{\mathbf{V}} \cdot \mathbf{N}$ is the normal speed of the points of \mathcal{S} , and σ_S is the entropy production at the interface.

As shown in (Maugin, 1997, 1998; Maugin and Trimarco, 1997), the entropy production can be expressed in terms of the “material” driving force f_S

$$f_S V_N = \theta_S \sigma_S \geq 0 \quad (12)$$

where θ_S is the temperature at S .

In addition, the balance of "material" forces at the interface between phases can be specified to the form (Maugin, 1997, 1998; Maugin and Trimarco, 1997)

$$f_S = -[W] + \langle \sigma_{ij} \rangle [\varepsilon_{ij}] \quad (13)$$

where W is the free energy per unit volume and ε_{ij} are the components of the strain tensor.

In the considered uniaxial case, we have

$$\begin{aligned} f_S = & -\frac{1}{2}[\sigma_{11}\varepsilon_{11}] - [\sigma_{12}\varepsilon_{12}] + \frac{1}{2}\frac{C}{\theta_0}[(\theta - \theta_0)^2] + \\ & + \frac{1}{2}[\alpha(3\lambda + 2\mu)(\theta - \theta_0)\varepsilon_{11}] + \langle \sigma_{11} \rangle [\varepsilon_{11}] + 2 \langle \sigma_{12} \rangle [\varepsilon_{12}] \end{aligned} \quad (14)$$

The surface balance equation (13) follows from the balance law for pseudomomentum (Maugin, 1993) and generalizes the equilibrium conditions at the phase-transition front to the dynamical case (c.f. Abeyaratne and Knowles, 1990, 1991, 1994; Maugin, 1997; Maugin and Trimarco, 1995; Truskinovsky, 1987, 1997).

2.2 The Impact Problem

In a dynamic problem we shall look for a piecewise smooth velocity and stress fields $v_2(x, t), \sigma_{12}(x, t)$ in inhomogeneous thermoelastic materials, which obey the following initial and boundary conditions:

$$\sigma_{12}(x, 0) = v_2(x, 0) = 0 \quad \text{for } 0 < x < L \quad (15)$$

$$v_2(0, t) = v_0 \quad \sigma_{12}(L, t) = 0 \quad \text{for } t > 0 \quad (16)$$

where v_0 is given constant, and satisfy the following field equations and jump conditions

$$\frac{\partial(\rho_0(\mathbf{x})v_2)}{\partial t} = \frac{\partial\sigma_{12}}{\partial x} \quad \frac{\partial}{\partial t} \left(\frac{\sigma_{12}}{\mu(\mathbf{x})} \right) = \frac{\partial v_2}{\partial x} \quad (17)$$

$$V_N[\rho_0 v_2] + [\sigma_{12}] = 0 \quad V_N[S] - \left[\frac{k}{\theta} \frac{\partial\theta}{\partial x} \right] = \sigma_S \geq 0 \quad [\mathbf{V}] = 0 \quad [\theta] = 0 \quad f_S V_N \geq 0 \quad \text{at } S \quad (18)$$

The field equations (17) are linear, but the whole problem is nonlinear because both position and velocity of a moving phase boundary should be determined inside the solution. Therefore, the initial-boundary value problem cannot be solved analytically, and we need to develop a numerical method capable of computing dynamical phase transition problems. We start with the wave-propagation algorithm (LeVeque, 1997) because the system of equations (17) is a system of conservation laws.

3 Finite-Volume Approximation

The system of equations for one-dimensional shear elastic wave propagation (17) can be represented in the form of a conservation law

$$\frac{\partial q}{\partial t} + \frac{\partial f(q, x)}{\partial x} = 0 \quad (19)$$

where

$$q(x, t) = \begin{pmatrix} \rho(x)v(x, t) \\ \sigma(x, t)/\mu(x) \end{pmatrix} \quad f(q, x) = \begin{pmatrix} -\sigma(\varepsilon, x) \\ -v(x) \end{pmatrix} \quad (20)$$

In the standard wave-propagation algorithm (LeVeque, 1997), the cell average

$$Q_n^k \approx \frac{1}{\Delta x} \int_{x_{n-1/2}}^{x_{n+1/2}} q(x, t_k) dx \quad (21)$$

is updated in each time step as follows

$$Q_n^{k+1} = Q_n^k - \frac{\Delta t}{\Delta x} (F_{n+1}^k - F_n^k) \quad (22)$$

where F_n^k approximates the time average of the exact flux taken at the interface between the cells, i.e.

$$F_n^k \approx \frac{1}{\Delta t} \int_{t_k}^{t_{k+1}} f(q(x_{n-1/2}, t)) dt \quad (23)$$

for each cell numbered by subscript n and each time step k .

The main difficulty here is to determine the appropriate values of numerical fluxes F_n^k . The corresponding procedure was established by LeVeque (1997) on the basis of the solution of the Riemann problems at each interface between cells. It was shown (Bale et al., 2002) that the characteristic property of the conservative wave-propagation algorithm is the following

$$F_{n-1}^+(Q_{n-1}^k) - F_n^-(Q_n^k) = f_n(Q_n^k) - f_{n-1}(Q_{n-1}^k) \quad (24)$$

where superscripts "+" and "-" denote numerical fluxes from the left and right sides of the cell edge, respectively. The advantages of the wave-propagation algorithm are high-resolution and the possibility for a natural extension to higher dimensions (Langseth and LeVeque, 2000). The wave-propagation method was successfully applied to the simulation of wave propagation in inhomogeneous media with rapidly-varying properties with some additional modifications to ensure the full second order accuracy (Fogarty and LeVeque, 1999).

What we need is to extend this well developed numerical method to the simulation of moving phase boundaries in solids. The required extension of the algorithm should be combined with the modelling of additional constitutive notions (kinetic relation and criterion of initiation) in the framework of thermodynamic consistency. The thermodynamic consistency manifests itself only at the discrete level of description (e.g., in numerical approximation). It simply means that the thermodynamic state of any discrete element (grid cell) of the computational domain should be consistent with the corresponding state of its sub-elements (sub-cells), if we try to refine the mesh.

3.1 Thermodynamics of Discrete Systems

It is salient to remind the reader of the notion of discrete systems in thermodynamics (Muschik, 1993). In such thermodynamics, the thermodynamic state space is extended by means of contact quantities in order to describe non-equilibrium states. In this perspective a discrete system is a domain G of \mathbf{R}^3 that is separated from its environment G^* by a contact surface ∂G . The interaction between G and G^* is described by contact quantities. In a Schottky system per se, this interaction consists of heat, work and mass exchanges. For instance, considering heat exchange \dot{Q} , the contact temperature is defined by the following inequality (Muschik, 1993):

$$\dot{Q} \left(\frac{1}{\Theta} - \frac{1}{T^*} \right) \geq 0 \quad (25)$$

for vanishing work and mass exchange rates. Here T^* is the thermostatic temperature of the equilibrium environment. From relation (25) it follows that \dot{Q} and the bracket have always the same sign. If we now suppose that there exists exactly one equilibrium environment for each arbitrary discrete system for which the net heat exchange between them vanishes, then the defining inequality (25) determines the contact temperature Θ of the system as the thermostatic temperature T^* of the system's environment for which this net exchange vanishes. The dynamic pressure, p , and the dynamic chemical potential, μ ,

are defined analogously

$$\dot{V} (p - p^*) \geq 0 \quad \dot{M} (\mu^* - \mu) \geq 0 \quad (26)$$

where \dot{V} is the time rate of volume, and \dot{M} is the time rate of mass. The contact quantities so defined provide a complete thermodynamic description of non-equilibrium states of a separated discrete system. Note, however, that the values of the defined contact quantities differ from the values of usual bulk parameters in the case of local equilibrium. For interacting elements, which are the case in our study, the values of bulk and contact quantities of adjacent elements are additionally connected by thermodynamic consistency conditions, which will be pointed out in the next section.

In the required extension of the concepts of the thermodynamics of discrete systems to the thermoelastic case, we divide the body into a finite number of identical elements. The state of each element is then identified with the thermodynamic state of a discrete system associated with that element, each element being assumed in local equilibrium. In thermoelasticity, in addition to Θ and the defining inequality (25), which governs heat exchange, we must define a contact dynamic stress tensor Σ_{ij} since the state space includes the deformation. Analogously to defining inequality (25) that holds for $\dot{\varepsilon}_{ij} = 0$ we have thus

$$\frac{\partial \varepsilon_{ij}}{\partial t} (\Sigma_{ij} - \sigma_{ij}^*) \geq 0 \quad (\dot{Q} = 0) \quad (27)$$

Here σ_{ij}^* is the Cauchy stress tensor in the environment. Now it remains to make the connection between the bulk quantities that appear in (17) and the defined contact quantities.

3.2 Thermodynamic Consistency Conditions

The thermodynamic consistency conditions for two simple thermodynamic fluid-like discrete systems, for which the internal energy \hat{E} depends only on the volume V and the temperature θ , i.e., $\hat{E} = \hat{E}(V, \theta)$, can be expressed as follows (Berezovski et al., 2000)

$$\left[\left(\frac{\partial(\hat{E} + \hat{E}^{int})}{\partial V} \right)_{\theta} \right] = 0 \quad (28)$$

in the homogeneous case (term "homogeneous" means here that the state of the system, combined by the two neighbouring systems, is determined under the assumption of continuity of temperature at the interface between the systems), and

$$\left[\left(\frac{\partial(\hat{E} + \hat{E}^{int})}{\partial V} \right)_{p} \right] = 0 \quad (29)$$

in the heterogeneous one (term "heterogeneous" means here that pressure is continuous across the interface). Remember that square brackets denote jumps of corresponding quantities. Here \hat{E}^{int} is the interaction energy, which appears in the description of the interaction of non-equilibrium discrete systems. The introduction of such an additional term is needed for the providing of a consistent simultaneous thermodynamic description of local accompanying states for both a discrete system as a whole and the same system combined by its discrete subsystems. It should be noted that the value of \hat{E}^{int} is undetermined, yet.

In the thermoelastic case, the thermodynamic derivatives which we should exploit instead of $\left(\frac{\partial \hat{E}}{\partial V} \right)_{\theta}$ and $\left(\frac{\partial \hat{E}}{\partial V} \right)_{p}$ are the following (Callen, 1960, ch.13.):

$$\left(\frac{\partial E}{\partial \varepsilon_{ij}} \right)_{\theta} = -\theta \left(\frac{\partial \sigma_{ij}}{\partial \theta} \right)_{\varepsilon_{ij}} + \sigma_{ij} \quad \left(\frac{\partial E}{\partial \varepsilon_{ij}} \right)_{\sigma_{ij}} = \theta \left(\frac{\partial S}{\partial \varepsilon_{ij}} \right)_{\sigma_{ij}} + \sigma_{ij} \quad (30)$$

where E is the internal energy per unit volume, and overbar denotes averaged quantities. It is supposed

that the introduced contact quantities are connected with the energy of interaction in a similar way

$$\left(\frac{\partial E^{int}}{\partial \varepsilon_{ij}}\right)_\theta = -\Theta \left(\frac{\partial \Sigma_{ij}}{\partial \theta}\right)_{\varepsilon_{ij}} + \Sigma_{ij} \quad \left(\frac{\partial E^{int}}{\partial \varepsilon_{ij}}\right)_{\sigma_{ij}} = \Theta \left(\frac{\partial S^{int}}{\partial \varepsilon_{ij}}\right)_{\sigma_{ij}} + \Sigma_{ij} \quad (31)$$

In fact, the latter two equations are relations of the constitutive type for the introduced contact quantities. However, the interaction entropy S^{int} is still undetermined yet.

Substituting the thermodynamic derivatives (30), (31) into the consistency conditions (28), (29), we obtain that the parameters of the adjacent non-equilibrium elements of a thermoelastic continuum should satisfy the thermodynamic consistency conditions, which can be called "homogeneous" (valid for all processes with no entropy production)

$$\left[-\theta \left(\frac{\partial \sigma_{ij}}{\partial \theta}\right)_{\varepsilon_{ij}} + \sigma_{ij} - \Theta \left(\frac{\partial \Sigma_{ij}}{\partial \theta}\right)_{\varepsilon_{ij}} + \Sigma_{ij}\right] = 0 \quad (32)$$

and "heterogeneous" (corresponds to any inhomogeneity accompanied by entropy production)

$$\left[\theta \left(\frac{\partial S}{\partial \varepsilon_{ij}}\right)_{\sigma_{ij}} + \sigma_{ij} + \Theta \left(\frac{\partial S^{int}}{\partial \varepsilon_{ij}}\right)_{\sigma_{ij}} + \Sigma_{ij}\right] = 0 \quad (33)$$

We propose to apply the thermodynamic consistency conditions to determine the values of field quantities at the phase boundary. However, we can develop a general procedure for the calculation of numerical fluxes at each interface between discrete elements.

For this purpose, we represent the finite-volume algorithm (22) in terms of contact quantities (Berezovski et al., 2000; Maugin and Berezovski, 2000; Berezovski and Maugin, 2001):

$$Q_n^{k+1} = Q_n^k - \frac{\Delta t}{\Delta x} (C_n^+(Q_n^k) - C_n^-(Q_n^k)) \quad (34)$$

where C^\pm denote contact quantities corresponding to the right and left interfaces of the element, respectively,

$$C^\pm(Q_n) = \begin{pmatrix} \Sigma^\pm(Q_n) \\ \mathcal{V}^\pm(Q_n) \end{pmatrix} \quad (35)$$

Here \mathcal{V} denotes, by duality, the contact deformation velocity. First we apply the homogeneous consistency condition (32) to determine the values of the contact quantities in homogeneous medium.

3.3 Contact Quantities in the Bulk

We distinguish "dynamic" and "thermal" parts of the condition (32) represented in terms of averaged bulk quantities, which are used in the finite-volume scheme (34):

$$[\bar{\sigma}_{ij} + \Sigma_{ij}] = 0 \quad \text{and} \quad \left[\bar{\theta} \left(\frac{\partial \bar{\sigma}_{ij}}{\partial \theta}\right)_{\varepsilon_{ij}} + \Theta \left(\frac{\partial \Sigma_{ij}}{\partial \theta}\right)_{\varepsilon_{ij}}\right] = 0 \quad (36)$$

In the homothermal case, it is sufficient to consider only the dynamic part. For the shear component in the uniaxial case, the dynamic part of the homogeneous consistency condition (36)₁ is reduced to

$$(\Sigma_{12}^+)_{n-1} - (\Sigma_{12}^-)_n = (\bar{\sigma}_{12})_n - (\bar{\sigma}_{12})_{n-1} \quad (37)$$

The latter should be complemented by the kinematic condition (Maugin, 1993) which can be rewritten in the small-strain approximation as follows

$$[\mathbf{v} + \mathbf{V}] = 0 \quad (38)$$

Assuming that the jump of contact velocity is determined by the second term of latter relation

$$[\mathcal{V}] = [\mathbf{V}] \quad (39)$$

we obtain in the uniaxial case

$$(\mathcal{V}_2^+)_{n-1} - (\mathcal{V}_2^-)_n = (\bar{v}_2)_n - (\bar{v}_2)_{n-1} \quad (40)$$

The two relations (37) and (40) can be expressed in the vectorial form as follows:

$$C_{n-1}^+(Q_{n-1}^k) - C_n^-(Q_n^k) = f_n(Q_n^k) - f_{n-1}(Q_{n-1}^k). \quad (41)$$

It is easy to see that the last expression is nothing more than the characteristic property (24) for the conservative wave-propagation algorithm.

Thus, the thermodynamic consistency conditions and kinematic conditions at the cell edge automatically lead to the conservative wave-propagation algorithm. From another point of view, this means that the wave-propagation algorithm is thermodynamically consistent.

In practice, we note that the contact velocities are connected with contact stresses by relations along characteristic lines of the system of equations (17)

$$(\mathcal{V}_2^-)_n = -\frac{(\Sigma_{12}^-)_n}{\rho_n c_n} \quad (\mathcal{V}_2^+)_{n-1} = \frac{(\Sigma_{12}^+)_{n-1}}{\rho_{n-1} c_{n-1}} \quad (42)$$

where $c^2 = \mu/\rho_0$.

Therefore, we have a linear system of equations for the determining of contact stresses

$$(\Sigma_{12}^+)_{n-1} - (\Sigma_{12}^-)_n = (\bar{\sigma}_{12})_n - (\bar{\sigma}_{12})_{n-1} \quad (43)$$

$$\frac{(\Sigma_{12}^+)_{n-1}}{\rho_{n-1} c_{n-1}} + \frac{(\Sigma_{12}^-)_n}{\rho_n c_n} = (\bar{v}_2)_n - (\bar{v}_2)_{n-1} \quad (44)$$

Solving the system of linear equations for contact stresses, we obtain the values of contact quantities needed to update the state of each cell to the next time step within the finite-volume numerical scheme (34).

The homogeneous consistency condition (32) was successfully applied in the composite wave-propagation algorithm for the simulation of thermoelastic wave propagation including the case of media with rapidly-varying properties (Berezovski et al., 2000; Maugin and Berezovski, 2000; Berezovski and Maugin, 2001). Moreover, the heterogeneous consistency condition (33) can be reduced to the homogeneous one for all processes with no entropy production. However, phase transitions are always accompanied by the production of entropy. This dictates us the rule of application of the consistency conditions: homogeneous one is used in the bulk (for thermoelastic waves) and the heterogeneous one is used at the phase boundary (where the entropy is produced).

3.4 Contact Quantities at the Phase Boundary

Suppose that the interface between two thermoelastic phases is placed between elements numbered by $p-1$ and p . We propose to apply the heterogeneous consistency conditions (33) for the calculation of the contact stresses at the phase boundary

$$\left[\bar{\theta} \left(\frac{\partial \bar{S}}{\partial \varepsilon_{ij}} \right)_{\sigma} \right] + [\bar{\sigma}_{ij}] + \left[\Theta \left(\frac{\partial S^{int}}{\partial \varepsilon_{ij}} \right)_{\sigma} \right] + [\Sigma_{ij}] = 0 \quad (45)$$

Further, we suppose that the jump of the entropy of interaction is equal to the jump of total entropy at the phase boundary

$$[S] = [S^{int}] \quad (46)$$

For the computation of the entropy jump at the phase boundary, we will exploit the jump relation corresponding to the balance of the entropy (11)₂ and the expression for the entropy production in terms of the driving force (12)

$$V_N[S] + \left[\frac{k}{\theta} \frac{\partial \theta}{\partial N} \right] = \frac{f_S V_N}{\theta_S} \quad (47)$$

where the driving force is determined by the balance of "material" forces (14). It follows from equations (46) and (47) that

$$[S] = \frac{f_S}{\theta_S} - \frac{1}{V_N} \left[\frac{k}{\theta} \frac{\partial \theta}{\partial N} \right] \quad (48)$$

Thus, we can conclude that the entropy of interaction has both thermal and dynamic contributions

$$S^{int} = S_{dyn}^{int} + S_{therm}^{int} \quad (49)$$

As previously, we divide the heterogeneous consistency condition (45) into dynamic and thermal parts. For the dynamic part we obtain

$$[\bar{\sigma}_{ij}] + [\Sigma_{ij}] = - \left[\theta \left(\frac{\partial S_{dyn}^{int}}{\partial \varepsilon_{ij}} \right)_{\sigma} \right] \quad (50)$$

Here we take into account that all the temperatures are equal in the homothermal case

$$\theta_{p-1} = \theta_p = \Theta_{p-1}^+ = \Theta_p^- \quad (51)$$

To compute the derivatives of the entropy of interaction with respect to thermodynamic variables ε_{ij} we extend the definition of the entropy of interaction on every point of the body by similarity to the relation (48):

$$S_{dyn}^{int} = \frac{f}{\theta} \quad (52)$$

where f is defined by analogy with the balance of material forces at the phase boundary (13)

$$f = -W + \langle \sigma_{ij} \rangle \varepsilon_{ij} + f_0 \quad (53)$$

with

$$\langle \sigma_{ij} \rangle = \frac{(\sigma_{ij})_p + (\sigma_{ij})_{p-1}}{2} \quad (54)$$

In the uniaxial case we have then for the shear contact stresses

$$(\Sigma_{12}^+)_{p-1} - (\Sigma_{12}^-)_p = 0 \quad (55)$$

This relation should be complemented by the coherency condition (10), which can be expressed in terms of contact velocities as follows

$$(\mathcal{V}_2^+)_{p-1} - (\mathcal{V}_2^-)_p = 0 \quad (56)$$

The contact velocities are still connected with contact stresses by the relations along characteristic lines of the system of equations (17). Therefore, the obtained conditions (55) and (56) form a linear system of equations which can be solved exactly. Thus, all the contact quantities at the phase boundary are determined, and we can update the state of the elements adjacent to the phase boundary by means of the wave-propagation algorithm. However, all the considerations are valid only after the initiation of the phase transformation process.

3.5 A Thermodynamic Initiation Criterion for the Stress-induced Phase Transition

We propose to expect the initiation of the stress-induced phase transition if both heterogeneous and homogeneous consistency conditions are satisfied at the phase boundary simultaneously. This is motivated by analogy with stability conditions in fluid-like systems.

In fact, the intrinsic stability of single-component simple systems may be expressed by two conditions (Callen, 1960, ch.8)

$$\left(\frac{\partial\theta}{\partial S}\right)_V > 0, \quad -\left(\frac{\partial p}{\partial V}\right)_\theta > 0 \quad (57)$$

If the criteria of stability (57) are not satisfied, then a system breaks up into two or more phases. The critical point that forms the boundary between full stability and instability is determined by several conditions, the first of them (necessary, but not sufficient) being the following (Callen, 1960, ch.9)

$$\left(\frac{\partial p}{\partial V}\right)_\theta = 0 \quad (58)$$

The same condition can be expressed in terms of the thermodynamic derivatives, which we use in the thermodynamic consistency conditions (28), (29)

$$\left(\frac{\partial\hat{E}}{\partial V}\right)_\theta = \left(\frac{\partial\hat{E}}{\partial V}\right)_p \quad (59)$$

The latter criterion can be interpreted as the condition of a continuous changing of the type of equilibrium.

Thus, we suppose that the heterogeneous consistency condition (33) and the homogeneous consistency condition (32) are simultaneously fulfilled at the phase boundary at the beginning of the phase transformation process

$$\left[\bar{\theta}\left(\frac{\partial\bar{S}}{\partial\varepsilon_{ij}}\right)_\sigma\right] + [\bar{\sigma}_{ij}] + \left[\bar{\theta}\left(\frac{\partial S^{int}}{\partial\varepsilon_{ij}}\right)_\sigma\right] + [\Sigma_{ij}] = 0 \quad (60)$$

$$[\bar{\sigma}_{ij}] - \left[\bar{\theta}\left(\frac{\partial\bar{\sigma}_{ij}}{\partial\theta}\right)_\varepsilon\right] + [\Sigma_{ij}] - \left[\bar{\theta}\left(\frac{\partial\Sigma_{ij}}{\partial\theta}\right)_\varepsilon\right] = 0 \quad (61)$$

Eliminating the jumps of stresses from the system of equations (60), (61), we again consider the dynamic part of the combined consistency condition

$$\left[\bar{\theta}\left(\frac{\partial}{\partial\theta}\left(\bar{\theta}\frac{\partial S^{int}}{\partial\varepsilon_{ij}}\right)_\sigma\right)_\varepsilon - \bar{\theta}\left(\frac{\partial S^{int}}{\partial\varepsilon_{ij}}\right)_\sigma\right] = 0 \quad (62)$$

For the shear component, the dynamic part of the combined consistency condition (62) leads to the continuity of the averaged shear stress at the phase boundary

$$[\bar{\sigma}_{12}] = 0 \quad (63)$$

Unfortunately, the latter relation can be fulfilled without any phase transformation (e.g., at rest). This is inconvenient for the criterion of the initiation of phase transformation process and we do not use it.

Thus, we still need a criterion for the initiation of the phase transformation process. For this purpose, we should check also the combined consistency condition (62) for the normal components which can be specified to the form

$$[f] \left\langle \frac{2(\lambda + 2\mu)}{\alpha(3\lambda + 2\mu)} \right\rangle + \langle f \rangle \left[\frac{2(\lambda + 2\mu)}{\alpha(3\lambda + 2\mu)} \right] = -[\theta_0^2 \alpha(3\lambda + 2\mu)] \quad (64)$$

Here we took into account that before the initiation of the phase transformation process all the temperatures hold the initial values

$$\theta_S = \theta_0 \quad (65)$$

Remember, that the value of f_0 is undetermined yet. We can choose this value in such a way that

$$\langle f \rangle = 0. \quad (66)$$

Therefore, we obtain for the driving force at the interface

$$f_S = [f] = -\frac{\theta_0^2}{2} [\alpha(3\lambda + 2\mu)] \left\langle \frac{\alpha(3\lambda + 2\mu)}{\lambda + 2\mu} \right\rangle \quad (67)$$

The right hand side of the latter relation can be interpreted as a critical value for the driving force. Therefore, the proposed criterion for the initiation of the stress-induced phase-transition in the case of uniaxial shear waves is the following one:

$$|f_S| \geq |f_{critical}| \quad (68)$$

where

$$f_{critical} = -\frac{\theta_0^2}{2} [\alpha(3\lambda + 2\mu)] \left\langle \frac{\alpha(3\lambda + 2\mu)}{\lambda + 2\mu} \right\rangle \quad (69)$$

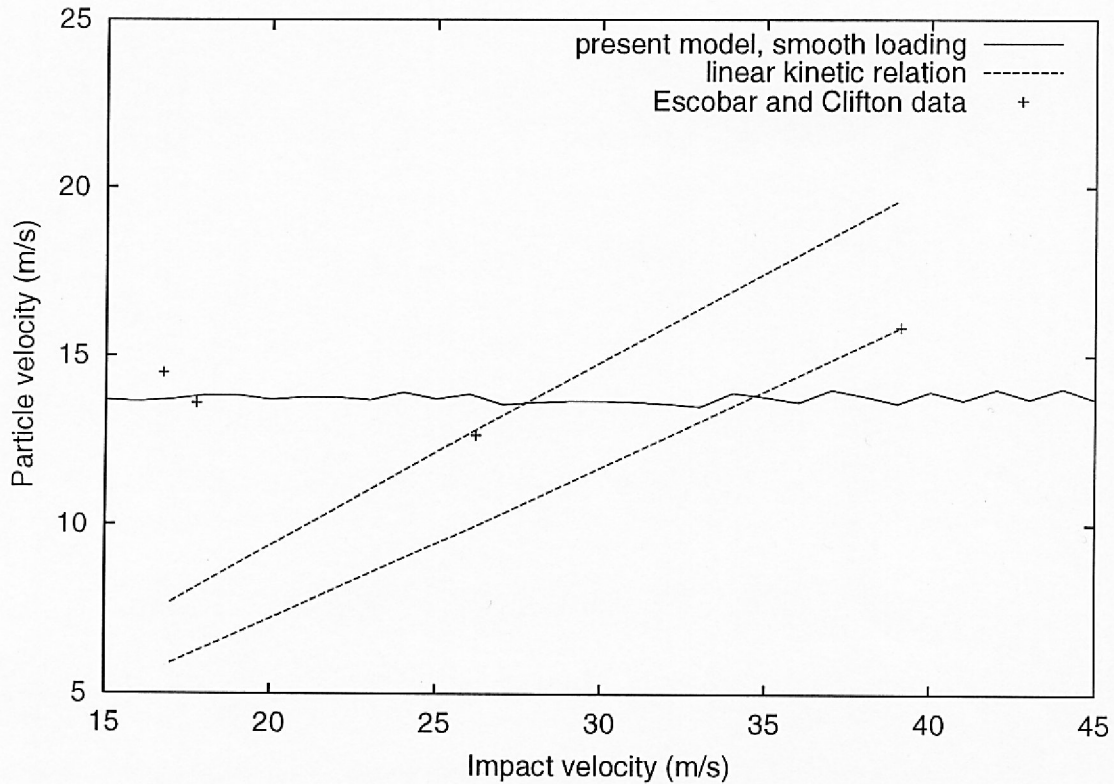


Figure 1. Particle Velocity versus Impact Velocity. Smooth Loading.

The material velocity at the interface is determined by means of the jump relation for linear momentum (11)

$$V_N^2 = \frac{[\bar{\sigma}_{12}]}{2 \langle \rho_0 \rangle [\bar{\epsilon}_{12}]} \quad (70)$$

The direction of the front propagation is determined by the positivity of the entropy production (12)

$$\sigma_S = \frac{f_S V_N}{\theta_S} \geq 0. \quad (71)$$

The obtained relations at the phase boundary are used in the described numerical scheme for the simulation of phase-transition front propagation.

4 Numerical Results

To compare the results of numerical simulation with experimental data by Escobar and Clifton (1993, 1995), we extract the properties of austenite phase of the Cu-14.44Al-4.19Ni shape-memory alloy from their paper: the density $\rho = 7100 \text{ kg/m}^3$, the elastic modulus $E = 120 \text{ GPa}$, the shear wave velocity $c_s = 2613.5 \text{ m/s}$, the dilatation coefficient $\alpha = 6.75 \cdot 10^{-6} \text{ 1/K}$. As it was recently reported (Emel'yanov et al., 2000), elastic properties of martensitic phase of Cu-Al-Ni shape-memory alloy after impact loading are very sensitive to the amplitude of loading. Therefore, for the martensitic phase we choose, respectively, $E = 60 \text{ GPa}$, $c_s = 2128 \text{ m/s}$, with the same density and dilatation coefficient as above. Following Abeyaratne and Knowles (2000), we note that the introduced elastic moduli are neither Young's moduli nor bulk moduli.

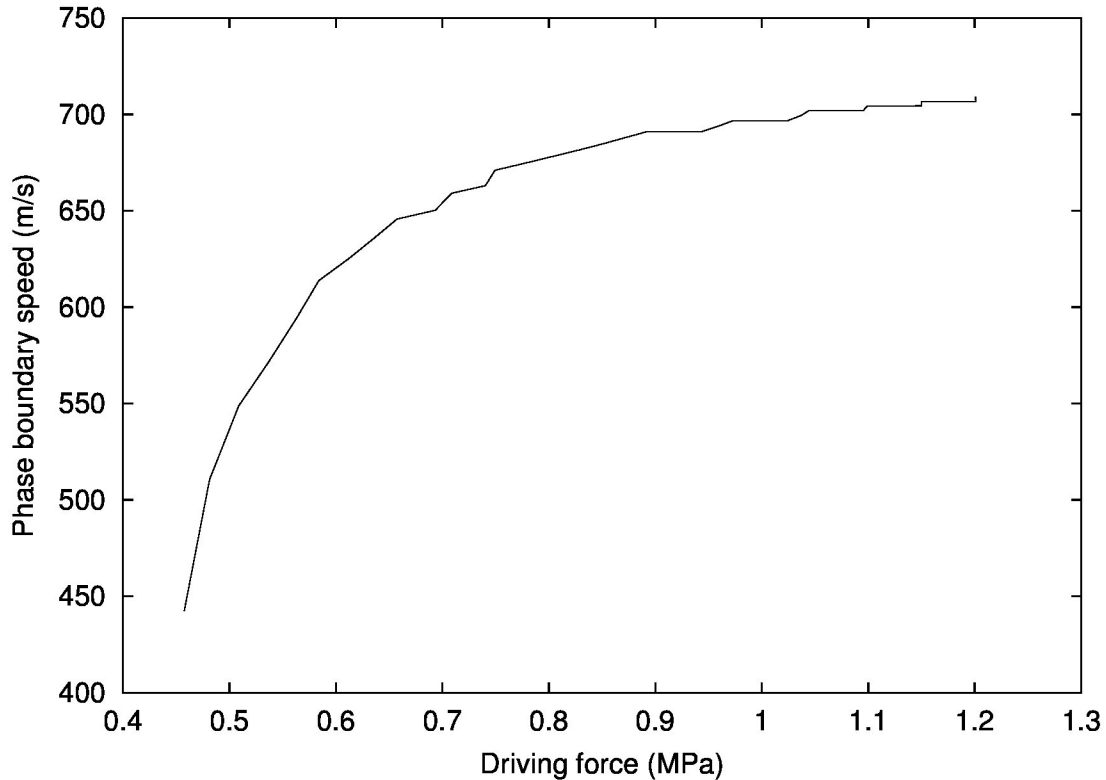


Figure 2. Kinetics of Transformation.

To compare the results of modelling with experimental data by Escobar and Clifton, we determined the particle velocities corresponding to different impact velocities. The calculations were performed by means of a composite finite-volume scheme with the Courant number equal to 1. In the homogeneous case this gives the exact solution of the hyperbolic system of equations (6).

Following Abeyaratne and Knowles (1997b), we use the half velocity of the flyer plate because the specimen and the flyer plate were both composed of the Cu-Al-Ni alloy being tested. The half of the measured transverse particle velocity is chosen for the comparison due to reflection at the rear face of the specimen. The results of the comparison are given in Fig. 1, where the predictions of the simple model corresponding to the linear kinetic relation (1) are also shown. It should be noted that the mobility coefficients in the linear model are calculated by means of the values of the driving force determined by the present numerical model and experimental data by Escobar and Clifton. As examples, two different

straight lines are given based on the results of two different experiments. As one can see, the linear models cannot approximate the experimental points related to remaining experiments. At the same time, the particle velocity computed by means of the present model is practically independent of the impact velocity, which has better correspondence to the available experimental data.

The kinetics of transformation can be represented by the relation between phase boundary speed and driving force, which is shown in Fig. 2. Here the corresponding values of the phase boundary speed are calculated by means of the relation (70), while the values of driving force are determined by the equation (14). As previously, the calculations were performed for different impact velocities. As one can see, the shape of the obtained curve is not linear. This confirms once more that linear kinetic relations are unable to predict the experimentally observed difference between tangential impact velocity and transversal particle velocity in the experiments by Escobar and Clifton.

Literature

1. Abeyaratne, R.; Knowles, J.K.: On the driving traction acting on a surface of strain discontinuity in a continuum. *J. Mech. Phys. Solids*, 38, (1990), 345 – 360.
2. Abeyaratne, R.; Knowles, J.K.: Kinetic relations and the propagation of phase boundaries in solids. *Arch. Rat. Mech. Anal.*, 114, (1991), 119 – 154.
3. Abeyaratne, R.; Knowles, J.K.: Dynamics of propagating phase boundaries: adiabatic theory for thermoelastic solids. *Physica D*, 79, (1994), 269 – 288.
4. Abeyaratne, R.; Knowles, J.K.: Impact-induced phase transitions in thermoelastic solids. *Phil. Trans. R. Soc. Lond.* A355, (1997a), 843 – 867.
5. Abeyaratne, R.; Knowles, J.K.: On the kinetics of an austenite-martensite phase transformation induced by impact in a Cu-Al-Ni shape-memory alloy. *Acta Mater.*, 45, (1997b), 1671 – 1683.
6. Abeyaratne, R.; Knowles, J.K.: On a shock-induced martensitic phase transition. *J. Appl. Phys.*, 87, (2000), 1123 – 1134.
7. Bale, D.S.; LeVeque, R.J.; Mitran, S.; Rossmanith, J.A.: A wave propagation method for conservation laws and balance laws with spatially varying flux functions, *SIAM J. Sci. Comp.*, (2002), (to be published).
8. Berezovski, A.; Engelbrecht, J.; Maugin, G. A.: Thermoelastic wave propagation in inhomogeneous media. *Arch. Appl. Mech.*, 70, (2000), 694 – 706.
9. Berezovski, A.; Maugin, G. A.: Simulation of thermoelastic wave propagation by means of a composite wave-propagation algorithm, *J. Comp. Physics*, 168, (2001), 249 – 264.
10. Callen, H.B.: *Thermodynamics*. Wiley & Sons, New York, 1960.
11. Emel'yanov, Y., et al.: Detection of shock-wave-induced internal stresses in Cu-Al-Ni shape memory alloy by means of acoustic technique. *Scripta mater.*, 43, (2000), 1051 – 1057.
12. Escobar, J.C.; Clifton, R.J.: On pressure-shear plate impact for studying the kinetics of stress-induced phase-transformations. *Mat. Sci. & Engng.*, A170, (1993), 125 – 142.
13. Escobar, J.C.; Clifton, R.J.: Pressure-shear impact-induced phase transformations in Cu-14.44Al-4.19Ni single crystals. In: *Active Materials and Smart Structures*, SPIE Proceedings, 2427, (1995), 186 – 197.
14. Fogarthy, T.; LeVeque, R.J.: High-resolution finite-volume methods for acoustics in periodic and random media, *J. Acoust. Soc. Am.*, 106, (1999), 261 – 297.
15. Fomethé, A.; Maugin, G.A.: Propagation of phase-transition fronts and domain walls in thermoelastic ferromagnets. *Int. J. Appl. Electromagn. Mech.*, 8, (1997), 143 – 165.
16. Langseth, J.O.; LeVeque, R.J.: A wave propagation method for three-dimensional hyperbolic conservation laws. *J. Comp. Physics*, 165 (2000), 126 – 166.
17. LeVeque, R.J.: Wave propagation algorithms for multidimensional hyperbolic systems. *J. Comp. Physics*, 131, (1997), 327 – 353.
18. Maugin, G.A.: *Material Inhomogeneities in Elasticity*. Chapman and Hall, London, 1993.

19. Maugin, G.A.: Thermomechanics of inhomogeneous - heterogeneous systems: application to the irreversible progress of two- and three-dimensional defects. *ARI*, 50, (1997), 41 – 56.
20. Maugin, G.A.: On shock waves and phase-transition fronts in continua. *ARI*, 50, (1998), 141 – 150.
21. Maugin, G. A.; Berezovski, A.: Thermoelasticity of inhomogeneous solids and finite-volume computations. In: *Contributions to Continuum Theories, Anniversary Volume for Krzysztof Wilmanski*, ed. B. Albers, Weierstrass Institute for Applied Analysis and Stochastics, Berlin, Report No. 18, 2000, 166 – 173.
22. Maugin, G.A.; Fomethé, A.: Phase-transition fronts in deformable ferromagnets. *Meccanica*, 32, (1997), 347 – 362.
23. Maugin, G.A.; Trimarco, C.: The dynamics of configurational forces at phase-transition fronts. *Meccanica*, 30, (1995), 605 – 619.
24. Maugin, G.A.; Trimarco, C.: Driving force on phase transition fronts in thermoelectroelastic crystals. *Math. Mech. Solids*, 2, (1997), 199 – 214.
25. Muschik, W. : Fundamentals of non-equilibrium thermodynamics. In: *Non-Equilibrium Thermodynamics with Application to Solids*. Ed. W. Muschik., Springer, Wien, 1993, 1 – 63.
26. Roytburd, A.L.: Principal concepts of martensitic theory. *J. de Physique IV*, 5, (1995), C8-21 – C8-30.
27. Truskinovsky, L.: Dynamics of nonequilibrium phase boundaries in a heat conducting nonlinear elastic medium. *J. Appl. Math. Mech. (PMM)*, 51, (1987), 777 – 784.
28. Truskinovsky, L.: Nucleation and growth in classical elastodynamics. In: P.M. Duxbury and T. Pence (Eds.) *Dynamics of Crystal Surfaces and Interfaces*, Plenum, New York, 1997, 185 – 197.

Addresses: Dr. Arkadi Berezovski, Department of Mechanics and Applied Mathematics, Institute of Cybernetics at Tallinn Technical University, Akadeemia tee 21, 12618, Tallinn, Estonia
e-mail: Arkadi.Berezovski@cs.ioc.ee
Prof. Gerard A. Maugin, Laboratoire de Modélisation en Mécanique, Université Pierre et Marie Curie, UMR 7607, Tour 66, 4 Place Jussieu, Case 162, F-75252, Paris Cédex 05, France
e-mail: gam@ccr.jussieu.fr